

B.K. DAS[✉]
H. SUCHE
W. SOHLER

Single-frequency Ti:Er:LiNbO₃ distributed Bragg reflector waveguide laser with thermally fixed photorefractive cavity

Angewandte Physik, Universität Paderborn, 33 098 Paderborn, Germany

Received: 7 June 2001

Published online: 30 October 2001 • © Springer-Verlag 2001

ABSTRACT The first single-frequency Ti:Er:LiNbO₃ distributed Bragg reflector waveguide laser with two thermally fixed photorefractive gratings as resonator mirrors is reported. The optically pumped ($\lambda_p = 1480$ nm, 120-mW incident power) laser emits up to 1.1 mW at $\lambda_s = 1561.1$ nm. The threshold pump power is 70 mW.

PACS 42.82.-m; 77.84.Dy; 76.30.Kg; 42.55.Rz; 42.40.Eq

1 Introduction

Integrable, single-frequency lasers are key components of dense wavelength-division multiplexed systems and of interferometric instrumentations. Er-doped LiNbO₃ devices are promising candidates as demonstrated by the recent developments of Ti:Er:LiNbO₃ distributed Bragg reflector (DBR) waveguide lasers using one narrow-band Bragg grating (etched or holographically written into LiNbO₃, sensitised by Fe-doping) and one broadband dielectric mirror deposited onto one polished waveguide end face [1, 2]. Although single-frequency operation could already be demonstrated with a laser using one etched surface-relief grating, this laser has a number of drawbacks: besides a complicated fabrication technology, etched gratings only weakly couple to the lasing mode due to a small overlap. Pumping through the grating is not possible due to coupling to substrate modes below the Bragg wavelength. Therefore, photorefractive gratings, as used in fibre-optic DBR and distributed-feedback lasers, are the more attractive alternative avoiding the drawbacks mentioned.

In this paper, we report the first single-frequency Ti:Er:LiNbO₃ DBR waveguide laser with two integrated, holographically written and thermally fixed photorefractive gratings in Ti:Er:LiNbO₃ waveguide sections forming the laser cavity (see Fig. 1). It is an improvement of the single-frequency device reported earlier, which had a DBR laser cavity comprising two photorefractive gratings as well; however only one was a fixed 'ionic' grating [3].

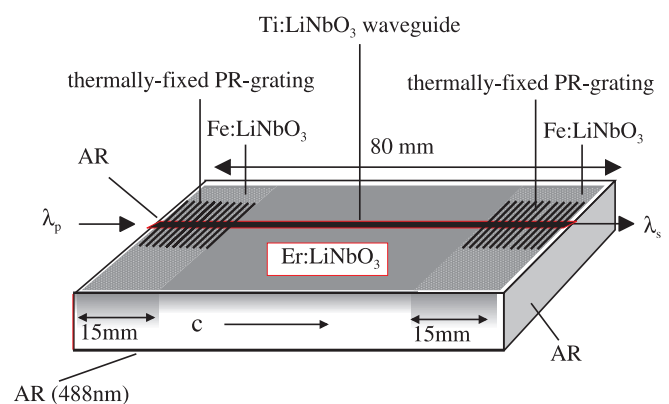


FIGURE 1 Schematic structure of the Ti:Er:LiNbO₃ waveguide laser with two DBR gratings in Fe-doped sections; AR: antireflection coating

2 Laser fabrication

The laser was fabricated in the surface of a 80-mm-long, 12-mm-wide and 1-mm-thick optical grade X-cut LiNbO₃ crystal. The *c* axis (optical axis) was along the longer side of the sample parallel to the propagation direction of the optical waveguides. The fabrication procedure started with two-step diffusion doping: the central amplifier section of the laser was Er-doped first, as its diffusivity is the lowest of all dopants used. Then the two outer sections were Fe-doped to increase the photorefractive sensitivity (Sect. 2.1). Afterwards, the optical waveguide was formed by Ti indiffusion (Sect. 2.2). Finally, the DBR laser cavity was fabricated by holographically writing two fixed photorefractive gratings (Sect. 2.3).

2.1 Diffusion doping of the substrate with erbium and iron

First, the middle section of 50-mm length of the substrate surface was Er-doped by indiffusion of a 19-nm-thick, vacuum-deposited Er layer at 1130 °C for 120 h. The resulting laser-active surface layer has a 1/e depth of the nearly Gaussian dopant profile of 4.4 μm. Besides the Er-doped section, an undoped part of the substrate was left to allow the fabrication of a reference waveguide.

✉ Fax:+49-5251/60-3422, E-mail: b.das@physik.uni-paderborn.de

Subsequently, the two remaining sections of 15-mm length on both ends of the substrate were Fe-doped by indiffusion of a 41-nm-thick vacuum-deposited Fe layer at 1060 °C for 72 h to increase the photorefractive sensitivity for the grating fabrication. The resulting (calculated) diffusion depth is 44.5 μm .

2.2 Waveguide fabrication and characterisation

Afterwards, a set of 7- μm -wide, 100-nm-thick, photolithographically defined Ti stripes parallel to the c axis and separated by 200 μm were indiffused (1060 °C, 7.5 h) to form the optical (single-mode) channel guides of about 4.5- μm ($1/e$) depth. Most of the waveguides have an Er-doped central section and Fe-doped outer sections (see Fig. 1), whereas a few channels in the undoped part of the sample serve as reference guides.

Finally, the end faces of the sample were polished perpendicular to the waveguide axis, resulting in low-finesse Fabry–Perot cavities. This allowed us to determine the waveguide scattering loss by analysing the contrast of the cavity resonances of the undoped reference guides [4]; the measured average loss was 0.10 (0.11) dB/cm for TE (TM) polarisation.

The absorption characteristics (see Fig. 2) of the Ti:Er:LiNbO₃ waveguide section was evaluated from the measured transmission of the light of a low-power broadband near-infrared light-emitting diode (LED). Both TE and TM modes showed similar absorption characteristics due to Z propagation. At the pump wavelength of 1480 nm the absorption is -7 dB.

Also, the gain characteristics was measured with 85 mW coupled pump power; both pump and signal were TE-polarised. A peak gain of ~ 7 dB at 1531-nm and ~ 3 dB at 1561-nm wavelength, respectively, was achieved (see Fig. 3). There were only small differences in the gain characteristics for other combinations of polarisations of pump and signal.

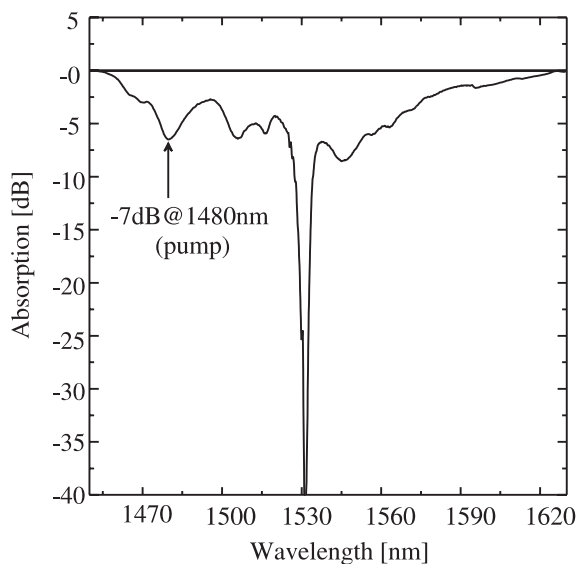


FIGURE 2 Absorption spectrum of 50-mm-long Ti:Er:LiNbO₃ waveguide section (TE polarisation)

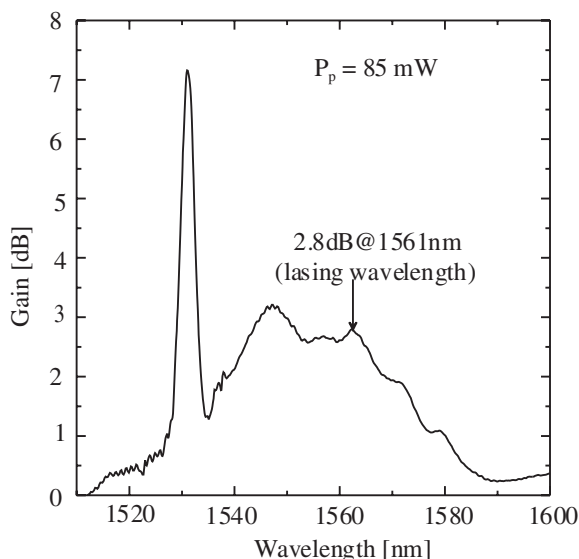


FIGURE 3 Gain characteristics of 50-mm-long Ti:Er:LiNbO₃ waveguide section; both pump and signal are TE-polarised

2.3 Photorefractive grating fabrication and characterisation

The sample was then annealed at 500 °C for 3 h in flowing Ar (0.5 l/min) to enhance in the outer waveguide sections the Fe²⁺/Fe³⁺ ratio, which determines the photorefractive sensitivity. The flowing Ar was bubbled through water to enhance also the H⁺ concentration, which is supposed to be responsible for thermal fixing of gratings [5, 6]. The back side of the sample was antireflection (AR)-coated for 488-nm radiation incident at about 45° to avoid reflections during grating fabrication. Finally, the end faces of the waveguide were AR-coated to improve the coupling of the pump and the laser output.

The grating was written with an argon-ion laser ($\lambda = 488$ nm, 1-W optical power) using the holographic setup shown in Fig. 4. It is evident that the periodic interference pattern was generated by wavefront division and subsequent superposition. The angle of incidence can be adjusted and determines the grating period of ~ 352 nm to get a Bragg reflection at $\lambda = 1561$ nm. The average intensity of the interference pattern on the waveguide surface was about 1 kW/cm², leading to writing times of less than 10 min. The growth

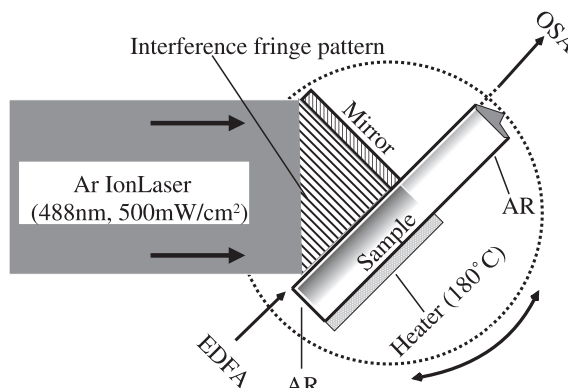


FIGURE 4 Holographic setup to fabricate fixed photorefractive gratings

of a grating was continuously observed by monitoring the spectrum of the transmitted amplified spontaneous emission of an erbium-doped fibre amplifier used as a broadband source.

The periodic illumination leads to a corresponding excitation of electrons from Fe²⁺ states; they are redistributed by drift, diffusion and mainly the photovoltaic effect, which is the dominant contribution along the optical *c* axis in the LiNbO₃ crystal. Finally, the electrons are trapped by Fe³⁺ acceptor states in the areas of low intensity. This redistribution generates a periodic space-charge field, which modulates the refractive index via the electro-optic effect and generates in this way a narrow-band Bragg-reflector grating.

However, a grating fabricated at room temperature is not stable over a long time due to a finite dark conductivity of electrons. Therefore, the gratings were written at 180 °C. At this temperature light positive ions, especially protons, become mobile and compensate the periodic electronic space charge [5]. After cooling the sample to room temperature within 5 min, these ions were frozen at their high-temperature positions. A subsequent homogeneous illumination with blue light at room temperature led to a nearly homogeneous redistribution of the electronic charge, developing in this way the stable 'ionic' grating of similar properties. Two such gratings were fabricated one after the other in the two Ti:Fe:LiNbO₃ sections of the sample. As a fixed 'ionic' grating can be easily erased at elevated temperatures (> 80 °C), it was thermally isolated by a carefully designed sample holder to allow writing of the second grating at 180 °C, while the first was kept at a temperature below 80 °C.

The transmission characteristics of the individual gratings are shown in Fig. 5 with nearly identical Bragg wavelengths near $\lambda_B = 1561.1$ nm. The reflectivity and line width of the high-reflection (HR) grating are 90% and 200 pm, respectively, whereas 60% and 60 pm were measured for the output coupler grating. These properties were observed when the gratings were homogeneously illuminated with light of an argon-ion laser ($\lambda = 488$ nm, $I = 100$ mW/cm²). When the

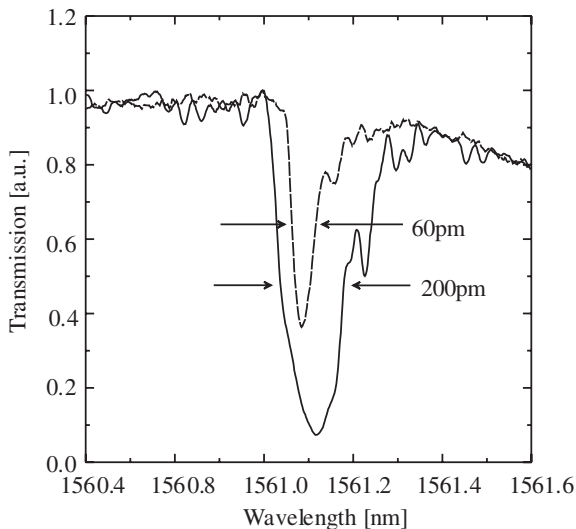


FIGURE 5 Transmission characteristics (TE mode) of fixed photorefractive gratings of the DBR cavity: *solid line*, high-reflection grating (HR); *dashed line*, output coupler grating

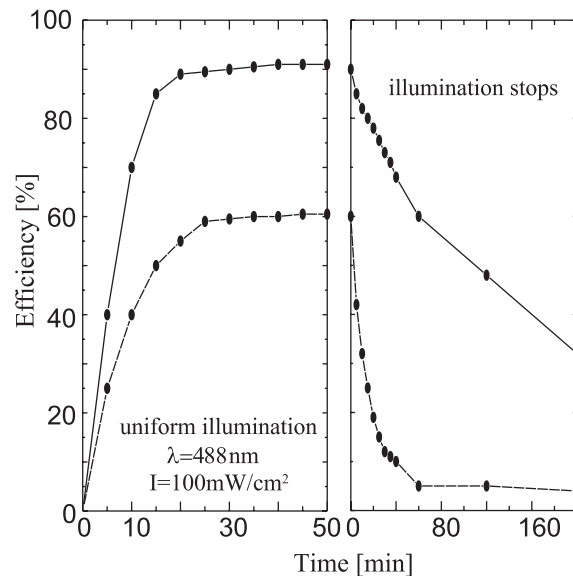


FIGURE 6 Development and decay characteristics of the gratings: *solid line*, high-reflection grating (HR); *dashed line*, output coupler grating

light was switched off, the grating efficiencies decayed with time in about 120 min (20 min) for the HR-(output coupler) mirror to half of their maximum responses due to a residual electronic conductivity leading to a compensation of the ionic charge distribution. However, it took only 20 min to refresh the gratings; they continued to keep their maximum efficiencies as long as they were illuminated (see Fig. 6). It was also possible to keep the gratings refreshed by the illumination from an array of blue GaN LEDs without any additional photorefractive damage.

3 Laser operation

The DBR waveguide laser was pumped using a pigtailed diode laser with an emission spectrum centred at ~ 1480 -nm wavelength, the optimum pump wavelength for α -polarisation ($\mathbf{E} \perp c$, $\mathbf{k} \parallel c$) in the LiNbO₃ waveguide. The pump light was fed into the laser resonator through the output coupler grating ($R = 60\%$) via the common branch of a fibre-optic wavelength-division demultiplexer (WDM) (see Fig. 7). The laser output was extracted through the second branch of the WDM and guided through an inline optical isolator to protect the DBR laser from optical feedback. During operation the two photorefractive gratings of the laser cavity were continuously illuminated by a uniform low intensity of Ar-laser light ($\lambda = 488$ nm, $I = 100$ mW/cm²).

The power characteristics of the laser are shown in Fig. 8. Lasing sets in at about 70-mW incident pump power measured at the output of the common branch of the WDM; the emission wavelength was 1561.1 nm. The laser was always running in TE polarisation independent of the pump polarisation (TE/TM). This might be due to the comparatively lower waveguide loss for the TE mode. With 120-mW incident pump power an output power of 1.1 mW was achieved, measured behind the isolator; the corresponding slope efficiency is about 2%.

Using a high-resolution optical spectrum analyzer (OSA) we could clearly identify that the DBR laser runs in a single

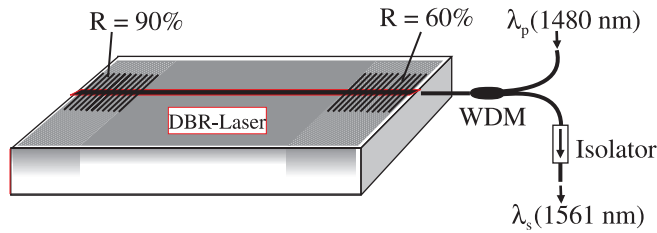


FIGURE 7 Schematic diagram of the DBR laser in operation

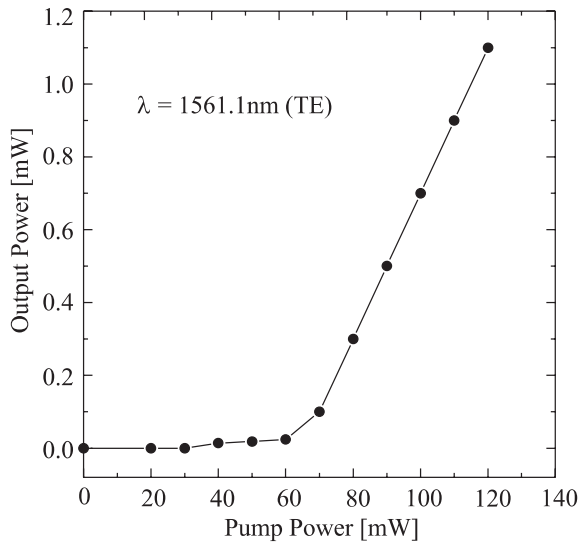


FIGURE 8 Laser output of the DBR laser vs. incident pump power ($\lambda_p = 1480$ nm; TE polarisation)

longitudinal mode of the cavity in TE polarisation (see Fig. 9). It was running for a duration of over half an hour without any observable wavelength fluctuations. The observed line width of ~ 0.75 GHz is clearly limited by the resolution of the OSA. A much better resolution (scanning Fabry–Perot or delayed self-heterodyne technique) is required to resolve the true laser line width of an estimated < 10 kHz as observed with a surface-etched device [7].

As the line width of the high-reflection grating is broader (200 pm) than that of the output coupler grating (60 pm), thermal tuning of the lasing wavelength was possible via the temperature of the output coupler alone (see Fig. 10). We achieved a tuning range of about 80 pm with a slope of 8 pm/°C. A wider tuning range can be obtained by additional temperature shift of the high-reflection grating.

The DBR laser will be packaged with GaN LED illuminated gratings to facilitate the further characterisation of the device and to investigate electro-optic tuning of the resonator.

4 Conclusions

We have demonstrated the first single-frequency Ti:Er:LiNbO₃ DBR waveguide laser with a monolithic integrated cavity comprising two fixed photorefractive Bragg gratings in Ti:Er:LiNbO₃ waveguide sections. Further optimisation of the cavity will lead to a higher output power and improved slope efficiency. Thermal and/or electro-optic tuning will allow us to develop a tunable single-frequency source

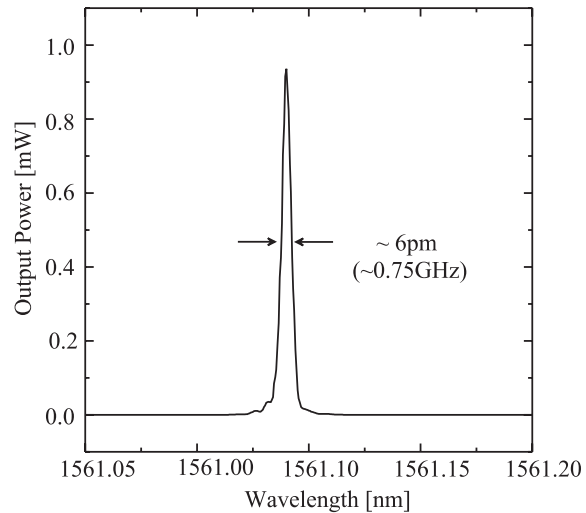


FIGURE 9 Spectral characteristics (TE polarisation) of the DBR laser

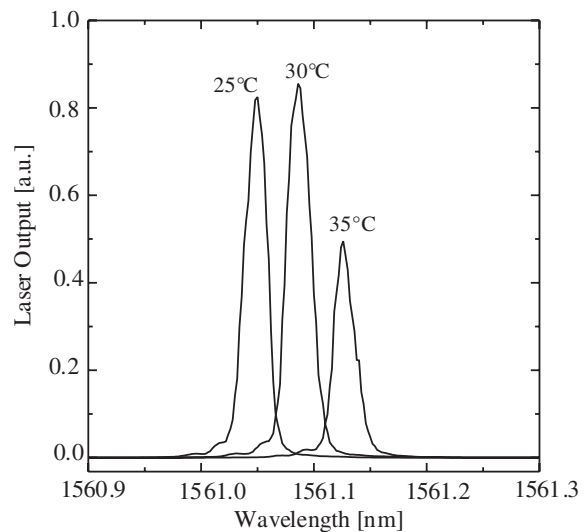


FIGURE 10 Tuning characteristics of the DBR laser; the HR grating is kept at room temperature, while the output coupler grating is temperature-tuned

in the future. It also seems that photorefractive gratings can be developed that do not require permanent refreshment [8].

ACKNOWLEDGEMENTS This work has been supported by the Deutsche Forschungsgemeinschaft as one project of the research group ‘Integrated Optics in Lithium Niobate: New Devices, Circuits and Applications’.

REFERENCES

- 1 J. Söchtig, R. Groß, I. Baumann, W. Sohler, H. Schütz, R. Widmer: *Electron. Lett.* **31**, 551 (1995)
- 2 C. Becker, A. Greiner, Th. Oesselke, A. Pape, W. Sohler, H. Suche: *Opt. Lett.* **23**, 1194 (1998)
- 3 B.K. Das, H. Suche, W. Sohler: *Proc. Eur. Conf. Integr. Opt. ECIO'01*, 2001, p. 87
- 4 R. Regener, W. Sohler: *Appl. Phys. B* **36**, 143 (1985)
- 5 J. Hukriede, I. Nee, D. Kip, E. Krätzig: *Opt. Lett.* **23**, 1405 (1998)
- 6 J.J. Amodei, D.L. Staebler: *Appl. Phys. Lett.* **18**, 540 (1971)
- 7 I. Baumann, S. Bosso, R. Brinkmann, R. Corsini, M. Dinand, A. Greiner, K. Schäfer, J. Söchtig, W. Sohler, H. Suche, R. Wessel: *IEEE J. Sel. Top. Quantum Electron.* **2**, 355 (1996)
- 8 J. Hukriede, D. Kip, E. Krätzig: *Appl. Phys. B* **72**, 749 (2001)